Brazilian Journal of Physics
ISSN: 0103-9733
luizno.bjp@gmail.com
Sociedade Brasileira de Física
Brasil

Continentino, Mucio Amado
Interplay of Quantum and Classical Fluctuations Near Quantum Critical Points
Brazilian Journal of Physics, vol. 41, núm. 2-3, septiembre, 2011, pp. 201-211
Sociedade Brasileira de Física
Sâo Paulo, Brasil

Braz J Phys (2011) 41:201–211
DOI 10.1007/s13538-011-0025-2

SOCIEDADE BRASILEIRA DE FÍSICA

CONDENSED MATTER

Interplay of Quantum and Classical Fluctuations Near Quantum Critical Points

Mucio Amado Continentino

Received: 9 June 2011 / Published online: 16 July 2011

Abstract For a system near a quantum critical point (QCP), above its lower critical dimension d_L, there is in general a critical line of second-order phase transitions that separates the broken symmetry phase at finite temperatures from the disordered phase. The phase transitions along this line are governed by thermal critical exponents that are different from those associated with the quantum critical point. We point out that, if the effective dimension of the QCP, $d_{\rm eff} = d + z$ (d is the Euclidean dimension of the system and z the dynamic quantum critical exponent) is above its upper critical dimension d_c there is an intermingle of classical (thermal) and quantum critical fluctuations near the QCP. This is due to the breakdown of the generalized scaling relation $\psi = \nu z$ between the shift exponent ψ of the critical line and the crossover exponent νz, for $d + z > d_c$ by a *dangerous irrelevant interaction*. This phenomenon has clear experimental consequences, like the suppression of the amplitude of classical critical fluctuations near the line of finite temperature phase transitions as the critical temperature is reduced approaching the QCP.

Keywords Strongly correlated electron systems · Critical point phenomena · Quantum phase transitions · Renormalization-group theory

M. A. Continentino (✉)
Centro Brasileiro de Pesquisas Físicas,
Rua Dr. Xavier Sigaud 150, 22290-180,
Rio de Janeiro, Rio de Janeiro, Brazil
e-mail: mucio@cbpf.br

1 Introduction

The modern theory of critical phenomena came to life four decades ago, when Wilson presented renormalization-group tools honed to deal with divergent free energies [1]. Soon applied to a number of classical second-order phase transitions, those tools determined the critical exponents associated with static properties, such as ν, associated with the divergence of the correlation length, or α, with the divergence of the specific heat, as well as the exponent z, associated with critical slowing down and necessary to describe dynamical properties.

Later, in the mid-1970s, a pair of developments extended the scope of the renormalization-group approach to quantum Hamiltonians. The first development started with two analyses of quantum models undergoing phase transitions [2, 3]. Young considered the d-dimensional Ising model subject to a transverse magnetic field h in the vicinity of the critical field h_c that destroys the magnetic order at zero temperature [2]. He showed that, at $T = 0$, the model mimics the classical $d + z$-dimensional Hamiltonian, where $z = 1$ is the dynamic exponent for the Ising model. At nonzero temperatures, by contrast, the critical behavior is that of the d-dimensional model with $h = 0$. To the same general conclusions came Hertz [3], who considered a broader class of models, including ones with $z > 1$. Quantum fluctuations intertwine the static and dynamical exponents; at the critical point, however, thermal fluctuations overcome them.

The second line of development was equally important. By the end of 1974, its remarkable record of successes notwithstanding, renormalization-group theory had covered but narrow regions of phase diagrams,

and some feared that it would never go beyond that. Fortunately, such fears were unfounded. The formalism had a great deal more power under its hood, which became visible when the Kondo Hamiltonian was diagonalized and its physical properties computed [4]. The Kondo model, a single impurity coupled to a Fermi gas, undergoes no phase transition; nonetheless, when a renormalization-group transformation was constructed, two fixed points became apparent, and it was shown that the unusual physical properties of the model reflect the crossover of the Hamiltonian from the high- to the low-temperature fixed point [4].

A decade later, when the same transformation was applied to the two-impurity Kondo problem, a quantum critical point (QCP) was identified at the meeting point of two competing tendencies: the coupling between each impurity and the Fermi gas, which tends to screen the impurity moment, and the antiferromagnetic interaction between the impurities, which tends to lock the impurity moments into a singlet effectively decoupled from the electron gas [5]. The fixed point associated with the QCP is analogous to the one discussed by Young [2]; in contrast with [2], however, [5] was able to extract the phase diagram for the two-impurity Kondo model from the renormalization-group streamlines.

The insight derived from that work offered an opportunity to perfect the then prevalent ideas concerning the phase diagram of the Kondo lattice. This realized, in a collaboration with Japiassu and Troper, the present author envisioned a hypothetical renormalization-group transformation, analogous to the one discussed in [5], argued that it should have two fixed points—a zero-temperature quantum fixed point and a nonzero temperature classical one (see Fig. 1, below, for an illustration)—and carried out a scaling analysis to discuss the renormalization-group flow of the model Hamiltonian in their vicinity [6].

Dependent only on basic assumptions, the scaling analysis proved to be as powerful as it is general. It offered an enlightening view of phase diagrams, one that pinpoints the origin of the singularities and affords easy derivation of scaling relations. Examples will be discussed below. Applied to the Kondo lattice, it showed that the quantum fixed point is unstable against thermal excitations and identified special renormalization-group flow lines stemming out of the unstable fixed point with boundaries in the phase diagram. More generally, the same construction provides insight and quantitative information on the behavior of such strongly correlated systems as the heavy-fermion and high-T_c compounds. Given the instability of the fixed point, renormalization-group flow lines are expected to emanate from the QCP and carry information about it even to points of the phase diagram that are distant from the quantum phase transition.

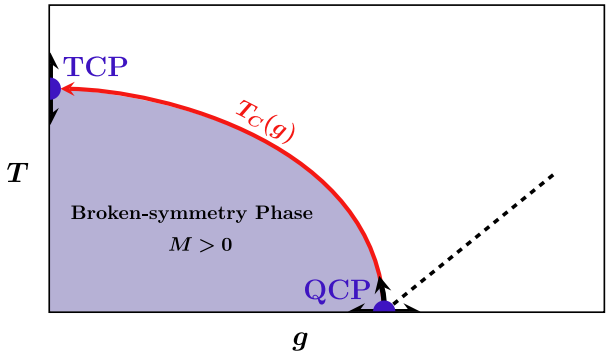

Fig. 1 Generic phase diagram for a quantum system above its lower critical dimension. As a function of the control parameter g, there is a quantum phase transition at the quantum critical point (*QCP*). There is also a critical line $T_C(g)$ of finite temperature phase transitions which is governed by a thermal critical point (*TCP*). The *arrows* show the flow of the renormalization-group equations

The recovery of that information is one of the exciting challenges in modern condensed-matter theory. This paper focuses that problem in a restricted domain of the phase diagram, the immediate vicinity of the QCP, and shows that, under conditions frequently found in the laboratory, thermal fluctuations may be damped by quantum fluctuations. Both the theoretical and the experimental facets of this finding are examined.

2 History

In the wake of [6], numerous studies of quantum phase transitions have been reported [7–18]. Experimentalists have studied the effects of such transitions on the finite temperature behavior of different physical quantities, some of which are noticeable even at unexpectedly high temperatures. Quantum phase transitions occur in a large variety of systems—metals, insulators, superconductors [7–9, 14, 16]—whenever a parameter can be tuned by external means to drive a system in or out of a broken-symmetry phase at zero temperature. Disorder can also be used as a control parameter [19, 20]. And the novel area of cold atom systems has opened broad new perspectives, since the strength of the interactions, which is generally fixed in condensed matter materials, can now be varied and used to explore different types

of phase diagrams close to a zero-temperature phase transition [16].

Theoretically, many techniques have been used to understand quantum phase transitions, such as simulations [11], different types of approximations [12, 21–24], scaling theories [6, 10], and the renormalization group, both in real [23–25] and momentum space [3, 12, 26]. These approaches yield the phase diagrams of the relevant models, the behavior of physical quantities, and the universality class of quantum critical points. In many cases, theory has been quite successful in explaining and even anticipating experimental results [6–9]. In certain situations, however, the experimental results seem to imply a dimensionality for the critical quantum fluctuations of the system that is different from that expected from its crystalline structure. This is the case of the ubiquitous logarithmic term in the specific heat of heavy fermions near an antiferromagnetic QCP. This logarithmic term arises in a $d = 2$, $z = 2$ universality class, but the systems showing this behavior are clearly three-dimensional [27], albeit anisotropic.

As explained above, a distinctive feature of quantum phase transitions is the inextricability of static and dynamics in critical phenomena [2, 3]. A clear manifestation of this entanglement between space and time fluctuations is the quantum hyperscaling relation [10], $2 - \alpha = \nu(d + z)$ where α and ν are standard critical exponents characterizing the non-analytic behavior of the free energy and the divergence of the correlation length, respectively [6]. The dimensionality of the system d appears in this relation modified by the dynamic exponent z. It is through this relation and the scaling of temperature near the QCP that the dynamic exponent enters the expression for the singular part of the free energy [28, 29]

$$f_S \propto |g|^{2-\alpha} F\left(\frac{T}{|g|^{\nu z}}, \frac{h}{|g|^{\beta+\gamma}}\right) \tag{1}$$

and ends up determining the critical behavior of static thermodynamical quantities. In (1), h is the field conjugate to the order parameter, β, its critical exponent, and γ, the critical exponent of the susceptibility. The parameter g measures the distance to the quantum phase transition occurring at $g = 0$. The appearance of the dynamic exponent in thermodynamic quantities is a unique feature of quantum phase transitions [28–30]. In particular, if the effective dimension $d_{\text{eff}} = d + z$ associated with a QCP is larger than its upper critical dimension d_c, the critical exponents describing the quantum critical behavior are Gaussian, or mean field exponents [3].

3 Classical and Quantum Critical Fluctuations

In Fig. 1, we show a schematic phase diagram of a system exhibiting quantum and thermal phase transitions. This phase diagram is typical of a quantum system above its lower critical dimensionality, i.e., a system with a broken-symmetry phase at finite temperatures. This can be recognized, for example, as the phase diagram of the two-dimensional Ising model in a transverse field resulting from a real space renormalization-group approach [25].

Classical and quantum critical phenomena are better described in the language of the renormalization group, which associates critical points with unstable fixed points of scaling transformations. The phase diagram of Fig. 1 contains a fully unstable zero-temperature fixed point, the QCP that controls quantum criticality, and a semi-unstable fixed point at finite temperatures, the thermal critical point (TCP) governing the classical critical behavior along the line of finite temperature phase transitions, $T_C(g)$. The arrows in Fig. 1 show the flow of the renormalization-group equations. In particular, the RG flow along the critical line is away from the QCP and toward the TCP.

In the figure, g is a control parameter such that $g = 0$ at the QCP. In the specific case of the transverse Ising model, $g = h - h_C$, with $h_C = (H/J)_C$, the critical ratio between the transverse field and the Ising interaction. The classical critical exponents are obtained from an expansion of the renormalization-group equations in the neighborhood of the thermal fixed point at the TCP. Since the RG flow along the critical line runs toward it, the TCP determines the critical behavior along the entire line. The QCP controls only the zero-temperature phase transition. However, as pointed out above, quantum fluctuations affect the finite-temperature physical properties making the properties of the QCP experimentally accessible, a point that will be further discussed below [8, 9, 31].

The phase diagram of Fig. 1 shows clearly a general feature of critical phenomena in quantum systems above their lower critical dimension d_L. Two universality classes coexist in the problem, related to the thermal and quantum phase transitions governed by the TCP and QCP, respectively. Expansions of the RG equations close to these fixed points yield different sets of critical exponents. In many cases of interest, the dimensionality d is smaller than the upper critical dimensionality d_C, while $d + z > d_C$; in such cases, the exponents of the QCP are mean field or Gaussian, while those describing the singularities along the critical line $T_C(g)$ are the Wilson exponents

associated with the TCP, which are much harder to determine.

4 Amplitude Relations Close to a Quantum Critical Point

For the sake of clarity, we choose to present the arguments in this section in the context of a real system showing both quantum and thermal phase transitions. The insulating antiferromagnetic material know as DTN [32, 33], with formula $NiCl_2$-4SC$(NH_2)_2$, presents two quantum phase transitions as a function of an external magnetic field, which have been shown to be due to a Bose–Einstein condensation of magnons. Also, it has a line of thermal phase transitions separating the broken-symmetry planar antiferromagnetic phase from the disordered paramagnetic phase.

A schematic temperature versus magnetic field phase diagram for this system is shown in Fig. 2. There are two QCPs at H_{C1} and H_{C2}, which are in the universality class of the density-driven three-dimensional Bose–Einstein condensation, with dynamic exponent $z = 2$ [32, 33]. On the other hand, the thermal phase transitions along the critical frontier separating the planar antiferromagnetic from the paramagnetic state are in the universality class of the classical three-dimensional XY model [34]. This is associated with a hypothetical finite-temperature three-dimensional XY fixed point, also shown in the figure, along with the expected RG flows.

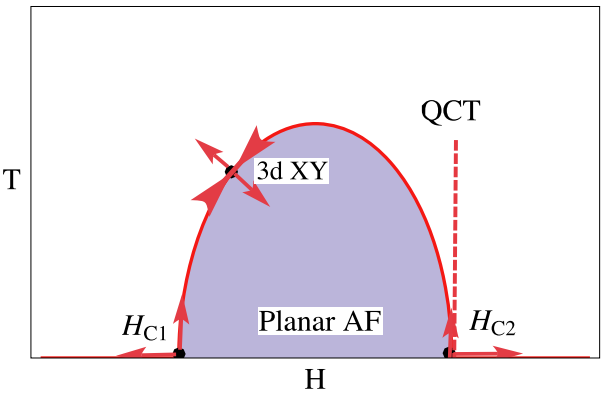

Fig. 2 Schematic phase diagram of the antiferromagnetic material $NiCl_2$-4SC$(NH_2)_2$. There are two QCPs at H_{C1} and H_{C2} which are in the universality class of the zero temperature density-driven three-dimensional Bose–Einstein condensation with dynamic exponent $z = 2$. The finite temperature transitions along the critical line belong to the universality class of the classical three-dimensional XY model. The *dashed line* is one of the quantum critical trajectories (QCT)

Consider the zero temperature Bose–Einstein condensation phase transition at the critical external magnetic field H_{C1}. A similar analysis can be carried out near H_{C2}. For small temperatures T, sufficiently close to the QCP, the critical line is given by $H_{C1}(T) = H_{C1}(1 + uT^{1/\psi})$ where u is a constant related to the magnon–magnon interaction [35] and ψ the *shift exponent*. Alternatively, the equation for this line close to H_{C1} can be written as $T_C(H) \propto |g|^{\psi}$, where $g = H - H_{C1}$.

For $d + z > 4$, the interaction u is a *dangerous irrelevant* quartic interaction [36, 37] acting on the Gaussian fixed point describing the QCP. It is *irrelevant* in the RG sense since it scales to zero close to this fixed point. It is *dangerously irrelevant* since it appears in the denominator of certain physical quantities, as shown below. It is responsible, in such cases, for breaking down the generalized scaling relation [26] $\psi = \nu z$.

Figure 2 shows that the flow of the RG equations at finite temperatures runs away from the QCP and toward the semi-stable three-dimensional XY fixed point (TCP). In the language of the RG, temperature is a *relevant field* which scales away from the zero temperature QCP. The flow is toward the semi-unstable TCP, which determines the thermal critical exponents. The latter, which describe the thermal phase transitions at $H_C(T)$ and are generally different from those associated with the QCPs, will be denoted by a *tilde* to distinguish them from the QCP critical exponents. We will thus refer to the quantum exponents as $\{\alpha, \beta, \gamma, \nu, z, \cdots\}$ and to the thermal critical exponents as $\{\tilde{\alpha}, \tilde{\beta}, \tilde{\gamma}, \tilde{\nu}, \cdots\}$.

In the first set, we emphasize the special role of the dynamic quantum critical exponent z, which appears in the expression for the free energy (1). The classical counterpart $\tilde{z}$ has no special significance, since it does not affect the critical behavior of static thermodynamic quantities.

In each set, the critical exponents are bound by scaling relations, for example, $\alpha + 2\beta + \gamma = 2$ and $\tilde{\alpha} + 2\tilde{\beta} + \tilde{\gamma} = 2$, which reduce the number of independent critical exponents. Particularly important is the hyperscaling relation involving the dimensionality d of the system. In the classical case, the hyperscaling relation is $2 - \tilde{\alpha} = \tilde{\nu} d$ [8, 9]. The quantum hyperscaling relation in turn involves the dynamic quantum critical exponent and is given by $2 - \alpha = \nu(d + z)$ [10]. The appearance of the effective dimension $d_{\text{eff}} = d + z$ has important consequences, for it decreases the upper *Euclidean dimension* d_C, above which the system is described by Gaussian or mean field exponents [8, 9]. In DTN, since the quantum phase transitions at H_{C1} and H_{C2} have $d_{\text{eff}} = d + z = 5 > d_c = 4$, both are described by Gaussian or mean field exponents [36, 37].

The above discussion appears to suggest that classical and quantum phase transitions in general have separate descriptions not interfering with each other. That this is not the case will be shown below, on the basis of a generalized scaling approach (GSA) [23, 24] extended for quantum phase transitions [31]. More specifically, we will see that, in the region of small nonzero temperatures in the neighborhood of the QCP, if the system is above its lower critical dimension $d_{\rm L}$ and presents a line of second-order thermal phase transitions, the description of the quantum and thermal critical behavior may involve, in each case, both quantum and thermal exponents.

In general, this occurs if the quantum phase transition is above its *upper critical dimension*, i.e., if $d+z \geq d_c$ and the generalized scaling relation $\psi = \nu z$ is violated due to a dangerous irrelevant interaction [26]—the magnon–magnon interaction in the BEC problem here considered [36, 37]. In this case, both quantum and thermal exponents are necessary to describe the physical behavior along the quantum critical trajectory (QCT), $T \to 0$ with $g = 0$.

For the Bose–Einstein condensation of magnons driven by an external magnetic field, the transverse susceptibility $\chi_\perp(H, T)$ plays the role of order parameter susceptibility. Close to the QCP at $H_{\rm C0}$ ($H_{\rm C0} = H_{\rm C1}$ or $H_{\rm C0} = H_{\rm C2}$), this susceptibility has the scaling form [8, 9]

$$\chi_\perp(H, T) \propto |g(T)|^{-\gamma} Q\left(\frac{T}{|g(T)|^{\nu z}}\right), \tag{2}$$

where $g(T) = |H - H_{\rm C}(T)|/H_{\rm C0}$ is the normalized distance to the critical line $g(T_{\rm C}) = 0$ and $H_{\rm C}(T) = H_{\rm C0}(1 + uT^{1/\psi})$ in the phase diagram.

Continuity imposes the following asymptotic behaviors on the scaling function $Q(t)$ ($t = T/|g(T)|^{\nu z}$) [8, 9, 38]:

- $Q(t = 0) =$ constant. This guarantees that at zero temperature, we obtain the correct expression for the quantum critical behavior of the transverse susceptibility, $\chi_\perp(H, 0) \propto |g|^{-\gamma}$, such that the order parameter susceptibility diverges at zero temperature with the quantum critical exponent γ.
- $Q(t \to \infty) \propto t^y$. The exponent $y = (\tilde{\gamma} - \gamma)/\nu z$ yields the correct thermal critical behavior of the transverse susceptibility close to the critical line $g(T) = 0$, i.e., $\chi_\perp(H, T) \propto A_\perp(T)|g(T)|^{-\tilde{\gamma}}$ as $T \to T_{\rm C}(H)$.

The amplitude $A_\perp(T) \propto T^{(\tilde{\gamma}-\gamma)/\nu z}$ is determined by both classical and quantum critical exponents. Then, close to the critical line, the order parameter susceptibility diverges as

$$\chi_\perp \propto A_\perp(T)\,|g(T)|^{-\tilde{\gamma}} \tag{3}$$

with the correct thermal critical exponent $\tilde{\gamma}$.

We now consider a special trajectory in the phase diagram of Fig. 2: We let the system *sit* at the QCP and lower the temperature. Along this QCT, $g(0) = 0$, i.e., for $H = H_{\rm C}(T = 0) = H_{\rm C0}$ and $T \to 0$, with help of the expression for the amplitude $A_\perp(T)$, we find from (3) that the transverse susceptibility diverges as,

$$\chi_\perp(H_{\rm C0}, T) \propto T^{\frac{\tilde{\gamma}-\gamma}{\nu z}} \left(uT^{\frac{1}{\psi}}\right)^{-\tilde{\gamma}}. \tag{4}$$

Then, it follows that for $d + z > d_c$ in the presence of a dangerous irrelevant interaction u breaking down the generalized scaling relation, such that $\psi \neq \nu z$, both thermal and quantum critical exponents are required to give the correct critical behavior along the QCT. Notice, however, that for $\psi = \nu z$, the exponent $\tilde{\gamma}$ cancels out in (4), and the divergence of the order parameter susceptibility, $\chi_\perp(H_{\rm C0}, T) \propto T^{-\gamma/\nu z}$, is governed only by the critical exponents associated with the QCP. The temperature dependence of this result coincides with that of a *purely Gaussian* ($u = 0$) theory, in which the quartic interaction u is neglected [8, 9]. The equality between the crossover and the shift exponents $\nu z = \psi$, i.e., the generalized scaling relation, is expected to hold for $d + z < d_c$.

For the correlation length, a similar analysis yields

$$\xi \propto A_L(T)|g(T)|^{-\tilde{\nu}} \tag{5}$$

with $A_L(T) = T^{(\tilde{\nu}-\nu)/\nu z}$. Along the quantum critical trajectory,

$$\xi(H_{\rm C0}, T) \propto T^{\frac{\tilde{\nu}-\nu}{\nu z}} \left(uT^{\frac{1}{\psi}}\right)^{-\tilde{\nu}}, \tag{6}$$

and in general, we find the same interference between classical and quantum critical behavior for $\psi \neq \nu z$. Again, for $\psi = \nu z$, the temperature dependence of $\xi(H_{\rm C0}, T)$ reduces to that of the purely Gaussian case, $\xi(H_{\rm C0}, T) \propto T^{-1/z}$. Notice in (4) and (6) that u appears in the denominator, justifying its dangerous irrelevant character. Equations (3) and (5) and their respective amplitudes give rise to a new effect, namely the *quantum suppression of classical fluctuations*, if the thermal exponents are non-Gaussian.

The specific heat requires a more careful analysis since it vanishes on the zero temperature axis. Its scaling behavior is obtained from the scaling expression for the singular part of the free energy close to the critical line, which is given by,

$$f_S \propto T^{\frac{\tilde{\alpha}-\alpha}{\nu z}} |g(T)|^{2-\tilde{\alpha}}. \tag{7}$$

The most singular contribution for the specific heat close to this line is given by

$$C/T \propto T^{\frac{\tilde{\alpha}-\alpha}{\nu z}} |g(T)|^{-\tilde{\alpha}} \left(g'(T)\right)^2, \tag{8}$$

where $g'(T) = \partial g/\partial T = -(uH_{C0}/\psi)T^{1/\psi-1}$. Along the QCT, if $\psi = \nu z$, the temperature dependence of this contribution coincides with that of the purely Gaussian result ($u = 0$) [8, 9], namely $C/T \propto T^{(d-z)/z}$.

We have used in this section a generalized scaling approach to show that for $\psi \neq \nu z$, the critical behavior of physical quantities in the neighborhood of a QCP from which emanates a line of second-order thermal phase transitions depends on both quantum and thermal exponents. Even along the quantum critical trajectory, $g = 0$, $T \to 0$, the classical and quantum critical behaviors are intermingled, provided only that $\psi \neq \nu z$.

5 Gaussian Approximations for the Classical Critical Behavior

The full problem schematized in Fig. 1 is of very difficult solution. The real space RG in general gives global phase diagrams and all the relevant fixed points in the problem [25]. Nonetheless, in this approach, it is hard to obtain controlled expansions that yield the correct critical exponents associated with these different fixed points. And for electronic systems, the real space RG has had only very limited success [8, 9]. Momentum-space RG [26] and self-consistent approximations [21, 22], on the other hand, give a better treatment of strongly correlated electronic systems. The former describes correctly the unstable fixed point associated with the QCP [26]; unfortunately it is limited to the neighborhood of the fixed point. Although it describes the correct temperature runaway flow away from the QCP, it fails to yield the thermal Wilson fixed point, to which the flow along the critical line is attracted.

The self-consistent approach [21, 22] is a Gaussian theory which yields the correct quantum critical exponents if the QCP effective dimension is larger than the upper critical dimension. However, it is inadequate to treat the thermal phase transitions and yields Gaussian thermal exponents.

In contrast with the limitations of other approaches, the GSA emerges as the perfect tool to understand the subtleties of quantum phase transitions. It is particularly useful to explore the intermingle of classical and quantum fluctuations near a QCP.

Both the momentum-space RG and the self-consistent approach to quantum phase transitions yield the shift exponent $\psi = z/(d + z - 2)$, showing clearly the breakdown of the scaling relation $\psi = \nu z$ for $d + z \geq d_c$. The momentum-space RG shows that this breakdown is due to a dangerous irrelevant quartic interaction acting on the Gaussian QCP. In the case of DTN, this is the magnon–magnon interaction u.

In this section, we show that the results of the momentum-space RG and of the self-consistent approach for the critical behavior along the quantum critical trajectory are recovered when we assume that the *thermal exponents* take thermal Gaussian values.

We are interested in the case $d + z \geq d_c$, i.e., in Gaussian *quantum critical exponents*. Consider (4) and (6) for the order parameter susceptibility and correlation length, respectively. Along the quantum critical trajectory, taking $\tilde{\gamma} = \gamma$ and $\tilde{\nu} = \nu$, we get for the order parameter susceptibility,

$$\chi_\perp \propto \left(uT^{\frac{1}{\psi}}\right)^{-\gamma} \tag{9}$$

and for the correlation length,

$$\xi \propto \left(uT^{\frac{1}{\psi}}\right)^{-\nu}, \tag{10}$$

which are the results from the momentum-space RG and self-consistent approach. These results are clearly distinct from those given in (4) and (6), respectively.

More importantly, the present analysis shows that substitution of Gaussian values for the thermal (*tilde*) critical exponents leads to temperature independent amplitudes, since the quantum exponents are Gaussian. This follows immediately from (3) and (5) and the corresponding amplitudes. Thus, if the thermal exponents turn out to be Gaussian, there will be no suppression of classical fluctuations in the vicinity of the QCP. This is illustrated in Figs. 3 and 4.

The analysis for the specific heat is much more subtle. Differently from other critical exponents, the quantum and thermal Gaussian exponents α and $\tilde{\alpha}$ are different and determined by the corresponding hyperscaling relations. For example, they yield $(\tilde{\alpha} - \alpha)/\nu z = 1$. We find that the most singular contribution to the specific heat arising from the free energy (7), assuming that the *tilde* exponents are Gaussian thermal exponents, is given by,

$$C/T \propto u^2 T^{\frac{2}{\psi}-1} |g(T)|^{-\tilde{\alpha}}. \tag{11}$$

Notice that in this case classical fluctuations are suppressed even with Gaussian thermal exponents ($\psi < 2$). Along the QCT, using $\tilde{\alpha} = 1/2$ in $d = 3$, we find that

$$C/T \propto u^{3/2} T^{\frac{3}{2\psi}-1}. \tag{12}$$

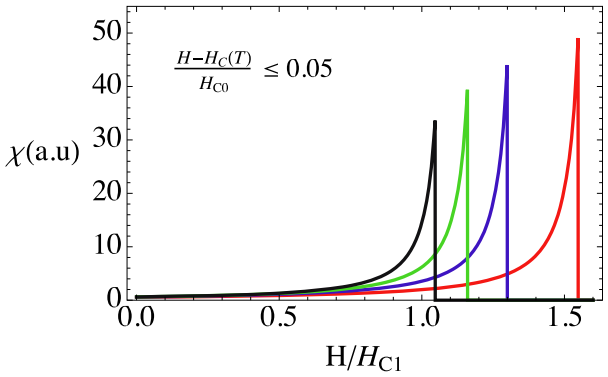

Fig. 3 The order parameter susceptibility close to the critical line $H_C(T)$ for fixed temperatures, assuming that the thermal exponents are those of the three-dimensional XY model. The *curves* have increasing temperature from *left* to *right* and extend to $(H - H_C(T))/H_{C0} = 5 \times 10^{-2}$. See Fig. 4 for comparison

Differently from (9) and (10) for the susceptibility and correlation length, the quartic interaction u appears in this case in the numerator. Equation (12) is the expected result for the specific heat along the QCT for $d = 3$, assuming that the thermal exponents are Gaussian and taking into account the dangerous irrelevant interaction u.

However, the purely Gaussian result [8, 9], which neglects the quartic interaction u ($u = 0$), namely $C/T \propto T^{(d-z)/z}$, is in general more singular as $T \to 0$ than the above contribution, (12). For the specific heat, whether we consider the purely Gaussian result, which neglects the interaction u, or (12), which takes u into account, we find that the most singular contribution determines the physical behavior along the QCT.

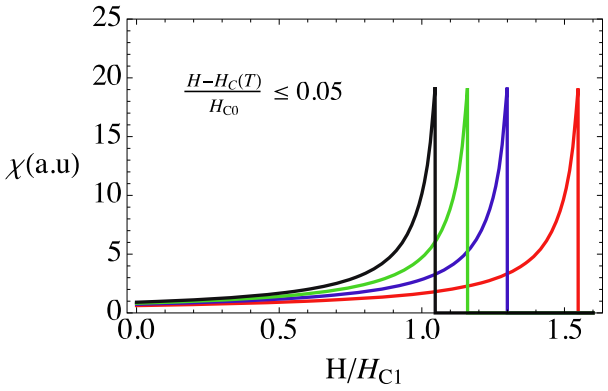

Fig. 4 The order parameter susceptibility close to the critical line $H_C(T)$ for fixed temperatures assuming Gaussian exponents for the thermal phase transitions. The *curves* have increasing temperature from *left* to *right* and extend to $(H - H_C(T))/H_{C0} = 5 \times 10^{-2}$

This follows from (11) and (12), the right-hand sides of which vanish for $u = 0$ and can be safely neglected with respect to the purely Gaussian ($u = 0$) contribution for the specific heat along the QCT. This is not the case for the susceptibility and the correlation length, which diverge for $u = 0$. Finally, we point out that the same temperature dependence of the pure Gaussian theory ($u = 0$) for C/T is obtained from (12), if we let $\psi = \nu z$ on the right-hand side.

6 Bose–Einstein Condensation in Magnetic Systems

One consequence of the difference between thermal and quantum critical exponents, as we have seen, is the suppression of the amplitude of critical fluctuations along the critical line as the critical temperature is reduced in the vicinity of a QCP. Besides, even along the quantum critical trajectory, the thermal exponents appear in the expressions for the critical behavior of different quantities. These are strong results with clear experimental consequences. In this section, we discuss the implication of these results for magnetic systems presenting a Bose–Einstein condensation of magnons as a function of the magnetic field.

This is the case of DTN, which has a phase diagram [32, 33] similar to that shown schematically in Fig. 2. As pointed out before, at H_{C1} and H_{C2}, the quantum phase transitions of this three-dimensional system are in the universality class of the density-driven Bose–Einstein condensation, with dynamic exponent $z = 2$. Since the effective dimension of the QCPs at these critical fields is $d_{\rm eff} = 3 + 2 = 5$, which is larger than $d_c = 4$, the quantum phase transitions are described by Gaussian or mean-field exponents. In particular, $\nu = 1/2$, so that $\nu z = 1$.

The shift exponent of the critical lines emanating from the QCPs is given by $\psi = z/(d + z - 2) = 2/3$, as results from the momentum-space RG analysis in [26]. This is clearly distinct from the crossover exponent $\nu z = z/2 = 1$. The dangerously irrelevant magnon–magnon interaction u is responsible for the breakdown of the scaling relation $\psi = \nu z$ in this case [36, 37]. The exponents we have just obtained describe well the critical behavior; in particular, $\psi = 2/3$ fits very well the critical lines close to the critical fields H_{C1} and H_{C2} [32–35, 39].

By contrast, the thermal or *tilde* exponents describing the thermal phase transitions along the finite temperature critical line are those of the three-dimensional XY model. These Wilson critical exponents are well-known [40–45]. They have been obtained by different

methods, from an RG ϵ expansion or numerical methods [40–43], and they have been verified experimentally [44, 45]. These thermal exponents are clearly distinguishable from the Gaussian exponents associated with the QCPs. The specific heat shows a clear λ anomaly at the critical line associated with a critical exponent $\tilde{\alpha} \approx 0$. We therefore have an opportunity to test the results in the previous sections.

Taking into account that the thermal critical exponents are different from the Gaussian exponents associated with the QCPs, we obtain a divergent order parameter susceptibility along the quantum critical trajectory, $\chi_\perp(H_{C0}, T) \propto u^{-\tilde{\gamma}/\psi} T^{-(1+\tilde{\gamma}/2)}$, where we used the Gaussian value for the susceptibility exponent of the QCP, $\gamma = 1$. Since $\tilde{\gamma} \approx 1.32$ for the three-dimensional XY model [40–45], this yields a contribution more singular than that of the momentum-space RG and self-consistent approach, namely $\chi_\perp(H_{C0}, T) \propto (uT)^{-\gamma/\psi} = (uT)^{-3/2}$.

For the specific heat, we find $C/T \propto u^2 T^{3/2} \log T$ along the quantum critical trajectory, $g(T = 0) = 0$, $T \to 0$. We used $\tilde{\alpha} \approx 0$ for the specific heat exponent of the three-dimensional XY model [40–45], which implies a logarithmic dependence in this case. However, this term is less singular than the purely Gaussian, order zero in u contribution to the specific heat, namely $C/T \propto T^{(d-z)/z} = T^{1/2}$.

Let us now investigate the behavior of the thermodynamic quantities at the critical line for sufficiently low temperatures near the QCPs. The influence of the quantum exponents due to the proximity of the quantum phase transition is contained in the expressions for the amplitude. Since the quantum critical exponents are Gaussian, we obtain for the thermal critical behavior of the order parameter susceptibility,

$$\chi_\perp(H, T) \propto T^{\tilde{\gamma}-1} \left| \frac{H - H_C(T)}{H_{C0}} \right|^{-\tilde{\gamma}} \tag{13}$$

and for the specific heat,

$$C/T \propto u^2 T^{\frac{3}{2}+\tilde{\alpha}} \left| \frac{H - H_C(T)}{H_{C0}} \right|^{-\tilde{\alpha}} \tag{14}$$

where for the three-dimensional XY model, $\tilde{\gamma} \approx 1.32$ and $\tilde{\alpha} \approx 0$ implying a λ-type anomaly for the specific heat [40–45] along the critical line. For completeness, we quote other critical exponents for the three-dimensional XY model, $\tilde{\nu} \approx 0.67$ and $\tilde{\beta} \approx 0.34$ [40–45].

For the analysis of the experimental data on the critical behavior along the critical line, we can adopt the following procedures. Suppose that, to approach the critical line in Fig. 2, we decrease the temperature for a fixed magnetic field $H_1 \gtrsim H_{C0}$. We then stop our measurements, say of the order parameter susceptibility, at a given arbitrary temperature T_1, distant from the thermal phase transition so that $[T_1 - T_C(H_1)]/H_{C0} = \delta$.

Next, we repeat the measurements for another fixed magnetic field $H_2 \gtrsim H_1$, stopping at another temperature T_2 distant from the critical line so that $[T_2 - T_C(H_2)]/H_{C0} = \delta$. When this procedure is repeated for several magnetic fields, we find from (13) that the susceptibility at the temperatures T_i such that $[T_i - T_C(H_i)]/H_{C0} = \delta$ is given by, $\chi_\perp(T_i) \propto T_i^{\tilde{\gamma}-1}\delta$ where δ is a fixed known constant. In this way, using the values of $\chi_\perp(T_i)$, we can determine the exponent $\tilde{\gamma}$.

Alternatively, we could increase the magnetic field at a fixed temperature T_1. We would then stop the measurements at a field H_1 distant from the thermal phase transition so that $[H_1 - H_C(T_1)]/H_{C0} = \delta$. We would repeat the measurement for another fixed temperature T_2 and stop at a distance from the critical line, such that $[H_2 - H_C(T_2)]/H_{C0} = \delta$. The susceptibility at the fields such that $[H_i - H_C(T_i)]/H_{C0} = \delta$ would then be given by $\chi_\perp \propto T_i^{\tilde{\gamma}-1}\delta$ where δ is a known constant.

Since, in practice, the susceptibility never diverges, we can take the temperatures T_i as the transition temperatures themselves. In this case, we can also work with the amplitudes given directly in terms of the magnetic field. Since $T_i = \left[(H_i - H_{C0})/uH_{C0}\right]^{\psi}$, substitu-

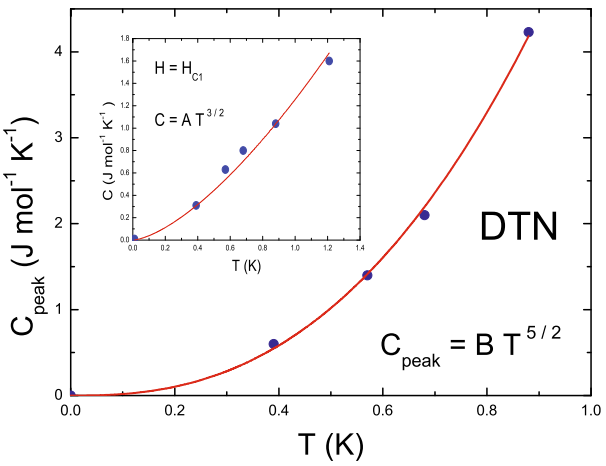

Fig. 5 The amplitude of the specific heat peaks at the finite temperature phase transitions into the planar antiferromagnetic order or Bose condensed phase of DTN. The *curve* is a plot of $C \propto T^{5/2}$ obtained using $\tilde{\alpha} \approx 0$ as appropriate for the three-dimensional XY model. The *inset* shows the specific heat at the QCP at H_{C1}. Points are data from [47]

tion on the right-hand side of (13) leads to $\chi_\perp(H_i) \propto \left[(H_i - H_{C0})/uH_{C0}\right]^{\psi(\tilde{\gamma}-1)}$. The envelope of the peaks in Fig. 3 is then the amplitude function.

We have carried out the procedure outlined above for the DTN system [32, 33] and also for $Sr_3Cr_2O_8$ [46], another magnetic system candidate for Bose–Einstein condensation [46]. The results for DTN are shown in Fig. 5 using the data near H_{C1} from [47]. The figure shows the specific heat at the peak temperatures, i.e., at the temperatures of the thermal phase transitions for different magnetic fields. The line through the points is $C \propto T^{5/2}$, as expected from (14) for $\tilde{\alpha} = 0$.

The fully Gaussian results, i.e., results obtained with thermal gaussian exponents, give a stronger suppression of the specific heat fluctuations namely, $C \propto T^3$. This seems to be the case for $Sr_3Cr_2O_8$, which is shown in Fig. 6; here, a T^3 law fits very well the amplitude of the specific heat in [46] for various magnetic fields close to the critical field. In this case, however, the T^3 dependence raises a doubt, for it is not clear whether we are observing critical fluctuations or measuring the phonon contribution to the specific heat.

In any case, $Sr_3Cr_2O_8$ is an isotropic magnetic system [46], unlike DTN, which has a condensed state of the XY type. In the inset of Fig. 5, we show the data for the specific heat of DTN along the QCT at H_{C1}. This follows approximately a $T^{3/2}$ behavior, in agreement with our conclusion that the purely Gaussian contribution ($u = 0$) $C/T \propto T^{(d-z)/z}$ dominates the thermal behavior of the specific heat.

Finally, we discuss the critical behavior of the longitudinal susceptibility $\chi_\parallel$ of the magnetic Bose system.

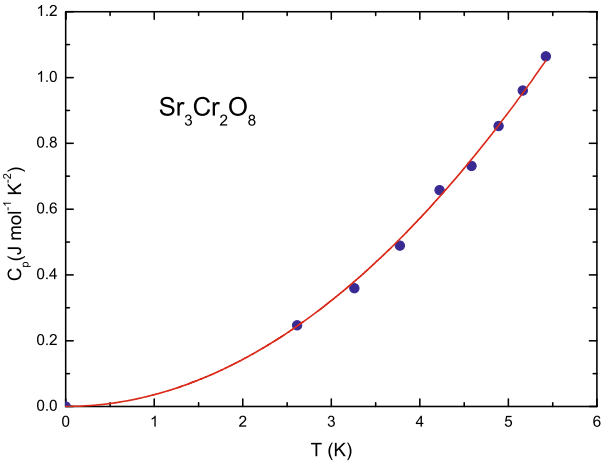

Fig. 6 The amplitude of the specific heat peaks at the finite temperature phase transitions in $Sr_3Cr_2O_8$. The curve is a plot of $C \propto T^3$ with $\tilde{\alpha} = 1/2$, as appropriate for the three-dimensional Gaussian model. Points are data from [46]

At zero temperature, $\chi_\parallel \propto \partial^2 f_S/\partial H^2$ scales as the compressibility of the Bose gas,

$$\chi_\parallel \propto |g|^{-\alpha} K\left[\frac{T}{|g|^{\nu z}}\right] \tag{15}$$

Notice that, in three dimensions, the quantum Gaussian exponent $\alpha = 2 - \nu(d+z) = -1/2$ is negative and the longitudinal susceptibility vanishes at the zero temperature phase transition. Mean field would give rise to at most a jump in the longitudinal susceptibility at the transition.

At $T = 0$ when the external magnetic field is larger than the upper critical field H_{C2}, the system is fully polarized and the scaling function $K(t = 0) = 0$. As temperature increases for $H > H_{C2}$ and below the line $T < T_G = |g|^{\nu z}$, this scaling function can be easily guessed, $K(t) = \exp(-T_G/T)$, since the system is gapped in this region of the phase diagram.

For finite temperatures, close to the critical line $H_C(T)$, we obtain $\chi_\parallel$ from the second derivative of the free energy with respect to the magnetic field. Using (7), we get,

$$\chi_\parallel \propto \frac{\partial^2 f_S}{\partial H^2} \propto T^{\frac{\tilde{\alpha}-\alpha}{\nu z}} \left|\frac{H - H_C(T)}{H_{C0}}\right|^{-\tilde{\alpha}} \tag{16}$$

Along the quantum critical trajectory, then, we get $\chi_\parallel \propto T^{(\tilde{\alpha}-\alpha)/\nu z}(uT^{1/\psi})^{-\tilde{\alpha}}$. For DTN we expect to find $\chi_\parallel \propto \sqrt{T}\ln T$ along the QCT, since $\tilde{\alpha} \approx 0$.

7 Discussion

Although discussed in the context of insulating magnetic systems presenting a Bose–Einstein condensation of magnons, the results in this paper should apply to any quantum phase transition. In particular, they also describe quantum criticality in metallic systems. For example, the equation for the amplitude of the specific heat at a thermal phase transition near a QCP,

$$C \propto T^{\frac{5}{2}}$$

holds near any superconductor quantum critical point with dynamic exponent $z = 2$ with the thermal superconductor transition in the universality class of the three-dimensional XY model.

The present approach relies only on universal features of continuous quantum phase transitions: We only assume that, near the transition, a characteristic length and a characteristic time contain all relevant information on the system. Any difference in the nature of the materials, whether metal or insulator, or in the phase transition itself, whether magnetic or superfluid, will

be accounted for by the various critical exponents, in special by the dynamic exponent z, which distinguish different universality classes.

8 Conclusion

We have used a generalized scaling approach to study the critical behavior of physical quantities near a quantum phase transition. We considered systems above their lower critical dimension, such that a line of finite-temperature continuous phase transitions emanates from the QCP. Our approach has shown that for quantum phase transitions described by Gaussian exponents, i.e., with $d + z > d_c$, where d_c is the upper critical dimension, classical and quantum fluctuations are intermingled near the QCP. The breakdown of the generalized scaling relation $\psi = \nu z$, between the shift and the crossover exponents, signals the intertwining. In general, this breakdown is due to a dangerous irrelevant interaction on the Gaussian fixed point describing the zero-temperature phase transition.

Our approach brings into the stage of quantum criticality the thermal phase transitions themselves. We find that thermal critical fluctuations close to a QCP are suppressed by quantum effects and their study allows a deeper understanding of quantum criticality. As future experiments progress toward lower temperatures, more detailed comparisons with theory will become possible allowing finer distinction between alternative scenarios.

We have shown that the momentum-space RG and the self-consistent approach yield quantum criticality results that follow from the GSA under the assumption of Gaussian exponents for the thermal phase transitions. Whether this is a sufficiently good description of the thermal phase transitions and, as implied by our analysis, of quantum criticality itself can be tested experimentally.

The alternative assumption that the thermal exponents have the expected Wilson character has stronger experimental consequences. The amplitude of critical thermal fluctuations will be reduced and the physical behavior along the quantum critical line will show deviations from the naively expected quantum critical exponents.

We found the behavior of the specific heat near the QCP to be different from that of other physical quantities such as, for example, the order parameter susceptibility, or the correlation length. The former has its amplitude suppressed near the QCP even assuming Gaussian thermal exponents. Besides, the corrections for this quantity due to the irrelevant interaction can safely be neglected when compared to the purely Gaussian ($u = 0$) result, which is more singular, in general. This is definitely not the case for other physical quantities, for which the corrections in u to the purely Gaussian result have u in the denominator due to its dangerously irrelevant character.

Acknowledgements I would like to thank Armando Paduan-Filho for useful discussions. I would like also to express my gratitude for the referee for suggestions and advices concerning the historical aspects of the development of the theory of quantum phase transitions. Work partially supported by Conselho Nacional de Desenvolvimento Científico e Tecnológico and Fundação de Amparo a Pesquisa do Estado do Rio de Janeiro.

References

1. K.G. Wilson, Phys. Rev. B **4**, 3174, 3184 (1971)
2. A.P. Young, J. Phys. C **8**, L309 (1975)
3. J.A. Hertz, Phys. Rev. B **14**, 1165 (1976)
4. K.G. Wilson, Rev. Mod. Phys. **47**, 773 (1975)
5. B.A. Jones, C.M. Varma, J.W. Wilkins, Phys. Rev. Lett. **61**, 125 (1988)
6. M.A. Continentino, G. Japiassu, A. Troper, Phys. Rev. B **39**, 9734 (1989)
7. S. Sachdev, *Quantum Phase Transitions* (Cambridge University Press, UK, 1999)
8. M.A. Continentino, *Quantum Scaling in Many-Body Systems* (World Scientific, Singapore, 2001)
9. M.A. Continentino, Phys. Rev. B **47**, 11587 (1993)
10. M.A. Continentino, G.M. Japiassu, A. Troper, J. Appl. Phys. **73**, 6631 (1993)
11. D.-X. Yao, J. Gustafsson, E.W. Carlson, A.W. Sandvik, Phys. Rev. B **82**, 172409 (2010)
12. S. Sachdev, Rev. Mod. Phys. **75**, 913 (2003), references therein
13. A.L. Fetter, Rev. Mod. Phys. **81**, 647 (2009)
14. Q. Si, F. Steglich, Science **329**, 1161 (2010)
15. J. Flouquet, G. Knebel, D. Braithwaite, et al., Compt. Rend. Phys. **7**, 22 (2006)
16. See *Pairing in Fermionic Systems*, ed. by A. Sedrakian, J.W. Clark, M. Alford (World Scientific, Singapore, 2006)
17. P.F. Bedaque, H. Caldas, G. Rupak, Phys. Rev. Lett. **91**, 247002 (2003)
18. H. Caldas, Phys. Rev. A **69**, 063602 (2004)
19. F. Evers, A.D. Mirlin, Rev. Mod. Phys. **80**, 1355 (2008)
20. A. Saguia, B. Boechat, M.A. Continentino, Phys. Rev. Lett. **89**, 117202 (2002)
21. T. Moriya, *Spin Fluctuations in Itinerant Electron Magnetism* (Springer, Berlin, 1985)
22. T. Moriya, T. Takimoto, J. Phys. Soc. Jpn. **64**, 960 (1995)
23. P. Pfeuty, R. Jullien, K.A. Penson, in *Real Space Renormalization Group* (Springer, Berlin, 1982), p. 119
24. R. Jullien, Can. J. Phys. **59**, 605 (1981)
25. R.R. dos Santos, J. Phys. C. Solid State Phys. **15**, 3141 (1982)
26. A.J. Millis, Phys. Rev. B **48**, 7183 (1993)
27. H.V. Löhneysen, et al., Phys. Rev. Lett. **72**, 3262 (1994)
28. M.A. Continentino, J. Physique I **1**, 693 (1991)
29. M.A. Continentino, Phys. Rev. B **47**(Rap. Comm.), 11587 (1993)
30. M.A. Continentino, Braz. J. Phys. **35**, 197 (2005)
31. M.A. Continentino, Solid State Commun. **75**, 89, (1990)

32. V.S. Zapf, D. Zocco, B.R. Hansen, M. Jaime, N. Harrison, C.D. Batista, M. Kenzelmann, C. Niedermayer, A. Lacerda, A. Paduan-Filho, Phys. Rev. Lett. **96**, 077204 (2006)
33. D. Reyes, A. Paduan-Filho, M.A. Continentino, Phys. Rev. B **77**, 052405 (2008)
34. L. Yin, J.S. Xia, V.S. Zapf, N.S. Sullivan, A. Paduan-Filho, Phys. Rev. Lett. **101**, 187205 (2008)
35. A. Paduan-Filho, K.A. Al-Hassanieh, P. Sengupta, et al., J. Appl. Phys. **105**, 07D501 (2009)
36. M.A. Continentino, JMMM **310**, 849 (2007)
37. M.A. Continentino, J. Phys. C: Cond. Matt. **18**, 8395 (2006)
38. P. Pfeuty, D. Jasnow, M.E. Fisher, Phys. Rev. B **10**, 2088 (1974)
39. Y. Kohama, A.V. Sologubenko, N.R. Dilley, V.S. Zapf, M. Jaime, J.A. Mydosh, A. Paduan-Filho, K.A. Al-Hassanieh, P. Sengupta, S. Gangadharaiah, A.L. Chernyshev, C.D. Batista, Phys. Rev. Lett. **106**, 037203 (2011)
40. W. Janke, Phys. Lett. **A148**, 306 (1990)
41. J.C. Le Guillou, J. Zinn-Justin, Phys. Rev. B **21**, 3976 (1980)
42. J.C. Le Guillou, J. Zinn-Justin, J. Phys. Lett. (Paris) **46**, L137 (1985)
43. M. Hasenbusch, S. Meyer, Phys. Lett. **B241**, 238 (1990)
44. L.S. Goldner, G. Ahlers, Phys. Rev. B **45**, 13129 (1992)
45. R. Reisser, R.K. Kremer, A. Simon, Physica **B204**, 265 (1995)
46. A.A. Aczel, Y. Kohama, C. Marcenat, 3.F. Weickert, M. Jaime, O.E. Ayala-Valenzuela, R.D. McDonald, S.D. Selesnic, H.A. Dabkowska, G.M. Luke, Phys. Rev. Lett. **103**, 207203 (2009)
47. Y. Kohama, A. Paduan-Filho, V. Zapf, P. Sengupta, C. Batista, M. Jaime, in *Specific Heat vs. Magnetic Field in* $NiCl_2$-$4SC(NH_2)_2$, National High Magnetic Field Laboratory 2009 Research Report. Available at http://www.magnet.fsu.edu/mediacenter/publications/reports/2009annualreport/2009-NHMFL-Report56.pdf